Multiple Domains in Caveolin-1 Control its Intracellular Traffic

Thomas Machleidt, Wei-Ping Li, Pingsheng Liu, and Richard G.W. Anderson

Department of Cell Biology, University of Texas Southwestern Medical Center, Dallas, Texas 75235-9039

Abstract. Caveolin-1 is an integral membrane protein of caveolae that is thought to play an important role in both the traffic of cholesterol to caveolae and modulating the activity of multiple signaling molecules at this site. The molecule is synthesized in the endoplasmic reticulum, transported to the cell surface, and undergoes a poorly understood recycling itinerary. We have used mutagenesis to determine the parts of the molecule that control traffic of caveolin-1 from its site of synthesis to the cell surface. We identified four regions of the molecule that appear to influence caveolin-1 traffic. A region between amino acids 66 and 70, which is in the most conserved region of the molecule, is necessary for exit from the endoplasmic reticulum. The region between amino acids 71 and 80 controls incorporation of caveolin-1 oligomers into detergent-resistant regions of the Golgi apparatus. Amino acids 91–100 and 134–154 both control oligomerization and exit from the Golgi apparatus. Removal of other portions of the molecule has no effect on targeting of newly synthesized caveolin-1 to caveolae. The results suggest that movement of caveolin-1 among various endomembrane compartments is controlled at multiple steps.

Key words: caveolae • membrane traffic • protein sorting • Golgi apparatus • endoplasmic reticulum

Introduction

Caveolin-1 was originally identified as a prominent tyrosine phosphorylated protein in Rous sarcoma virus transformed cells (Glenney, 1989; Glenney and Zokas, 1989). The localization of the protein to caveolae striated coat material (Rothberg et al., 1992) initiated a program of study to determine its function in this membrane domain. Initially, it was thought that caveolin-1 might be a coat protein, similar in design to clathrin or coatomer. However, cloning and sequencing of the caveolin-1 cDNA showed that it most likely was an integral membrane protein inserted so that both ends of the molecule are in the cytosol (Anderson, 1998) and that it did not have homology to any coat proteins. Coimmunoprecipitation assays indicate that caveolin-1 can interact with a variety of peripheral and integral membrane proteins (Okamoto et al., 1998). Some of these interactions appear to involve the 33-amino acid (aa)[1] long hydrophobic region that is thought to insert the protein into the lipid bilayer (Wary et al., 1996; Das et al., 1999). Biochemical studies have shown that a 20-aa sequence (aa 80–100) proximal to the membrane insertion region interacts with a broad range of signal transducing molecules, including tyrosine kinase receptors, endothelial nitric oxide synthase (eNOS), and heterotrimeric G proteins (for review see Okamoto et al., 1998). This so-called scaffolding domain was used to isolate from a phage display library a peptide motif (ϕ-X-ϕ-X-X-X-ϕ, ϕ-X-X-X-X-ϕ-X-X-ϕ, or ϕ-X-ϕ-X-X-X-X-ϕ-X-X-ϕ) that is found in several of the molecules that interact with caveolin-1. The scaffolding domain does not appear to be involved in targeting integral membrane proteins to caveolae (Mineo et al., 1999), but may play a role in modulating signal transduction at this site (Okamoto et al., 1998).

Caveolin-1 also has an important function in intracellular cholesterol traffic. This isoform of caveolin is a cholesterol (Murata et al., 1995) and fatty acid (Trigatti et al., 1999) binding protein that appears to be upregulated in response to increased levels of cellular cholesterol (Fielding et al., 1997; Hailstones et al., 1998). Expression of caveolin-1 in cultured lymphocytes that ordinarily lack the protein markedly accelerates the rate of cholesterol transport from the ER to the plasma membrane (Smart et al., 1996). At the same time, the caveolae membrane fraction becomes enriched in cholesterol and the number of invaginated caveolae in the cell increases (Fra et al., 1995). Therefore, caveolin-1 appears to play a role in maintaining the proper level of cholesterol in caveolae.

Caveolin-1 is found in the Golgi apparatus (Luetterforst et al., 1999) and at the cell surface (Rothberg et al., 1992) of most normal tissue culture cells. As much as 90% of the cellular caveolin-1 is at the cell surface (Das et al., 1999), and immunogold labeling indicates that the majority of

---

this pool is localized to caveolae (Rothberg et al., 1992). Some of the Golgi-associated caveolin-1 is in transit from its site of synthesis in the ER (Monier et al., 1995) to the cell surface. Indeed, the Golgi apparatus may be a site of caveolae assembly (Lisanti et al., 1993). Surface caveolin-1 also recycles through the Golgi apparatus using a novel pathway that involves the direct movement of the molecule from caveolae to the lumen of the ER and on to the Golgi apparatus (CERGA) (Conrad et al., 1995; Smart et al., 1994). A cytoplasmic pool of caveolin-1 that is in a complex with multiple chaperones may be an intermediate in the CERGA pathway (Uittenbogaard et al., 1998). Finally, caveolin-1 probably recycles in caveolae vesicles returning to the cell surface after internalization during potocytosis (Parton et al., 1994).

Immunofluorescence cannot distinguish between the recycling and the newly synthesized pools of caveolin-1 in the Golgi apparatus. One potential distinguishing feature of the CERGA pathway is that the caveolin-1 in the ER and Golgi apparatus is not intercalated into membranes, and therefore behaves like a soluble protein (Smart et al., 1994). It is also not degraded when cell homogenates are treated with proteases. On the other hand, the caveolin-1 that has been incorporated into nascent caveolae in the Golgi apparatus is in a high molecular weight complex (Lisanti et al., 1993) that is resistant to detergent solubilization (Scheiffele et al., 1998). The caveolin-1 in the Golgi apparatus is either in route to the cell surface from its site of synthesis in the ER, or has arrived from a recycling pathway.

The dynamic behavior of caveolin-1 must depend on specific domains within the protein that control its intracellular traffic. These domains contain sorting information that specifies how the molecule will transit from the ER to the cell surface as well as its recycling itinerary. In an attempt to identify some of these codes, we have expressed multiple mutant forms of caveolin-1 and analyzed the traffic pattern for each in a cell that normally expresses the protein. We now report on the identification of four regions in the molecule that control different stages of caveolin-1 intracellular traffic.

Materials and Methods

Materials

Polyclonal antibody (pAb) Myc was purchased from Upstate Biotechnology, Inc. pAb caveolin-1 and mAb caveolin-1 number 2234 were purchased from Transduction Laboratories. Anti–mannosidase II antiserum was provided by Dr. Moremen (University of Georgia, Athens, GA). mAb grp78 was obtained from StressGen. Alexa 488 goat anti–rabbit IgG and Alexa 568 goat anti–mouse IgG were purchased from Molecular Probes. Isopropyl-β-D-thiogalactoside (IPTG) was purchased from Calbiochem and kept at −20°C (stock solutions 200 mM in H_2O). BSA, proline, leupeptin, soybean trypsin inhibitor, pepstatin A, and benzamidine were from Sigma Chemical Co. Lipofectamine Plus and G418 were from GIBCO BRL.

Protease inhibitors were stock solutions (1,000×) of benzamidine (500 mM in H_2O), leupeptin (10 mM in H_2O), trypsin inhibitor (10 mg/ml in H_2O), and pepstatin (1 mg/ml in methanol). Buffers A–E consisted of the following. Buffer A: 100 mM sodium phosphate, pH 7.4, 0.15 M NaCl, 4 mM KCl, 2 mM $MgCl_2$, and 0.02% (wt/vol) sodium azide; buffer B: 25 mM MES, pH 6.5, 150 mM NaCl, 1:1,000 dilution of each protease inhibitor; buffer C: 25 mM MES, pH 6.5, 150 mM NaCl, 1% Triton X-100, 1:1,000 dilution of each protease inhibitor; buffer D: 20 mM Tris, pH 8.0, 150 mM NaCl, 1% Triton X-100, 60 mM octylglucoside, 1:1,000 dilution of each

protease inhibitor; and buffer E: 0.25 M sucrose, 20 mM Tricine, pH 7.8, 1 mM EDTA, 1:1,000 dilution of each protease inhibitor.

Cell Culture

CHO-K2 and CHO-K2 lacRep cells were kindly provided by Dr. Michael Roth (Department of Biochemistry, University of Texas Southwestern Medical Center, Dallas, TX). CHO-K2 lacRep is a stable transfected CHO-K2 line expressing the lac repressor under control of the cytomegalovirus (CMV) promoter. The expression of the lac repressor was verified by immunofluorescence using a lac repressor pAb. The cells were maintained in DME supplemented with 10% FCS and 20 μg/ml proline in a humidified incubator at 37°C and 5% CO_2. Cells were grown in 100-mm cell culture dishes until ~70–80% confluent before inducing the expression of individual constructs by incubating the cells in the presence of 5 mM IPTG for 16 h. Transfected cells were never maintained in culture longer than 10–12 wk before replacing them with fresh cells.

Construction of Normal and Mutant Caveolin-1 cDNA

A series of mutations in caveolin-1 were generated by PCR from the original cDNA clone of α-caveolin-1 (see Fig. 1) using the Expand High Fidelity PCR system (Roche). The PCR products were subcloned into the EcoRI and HindIII sites of pCDNA3-lacRep-MycHis, a derivative of pCDNA3-MycHis generated by excising the CMV promoter with BglII and NotI and inserting the promoter region of pCMV3lacRep (Welch et al., 1998). This region contains the CMV promoter with multiple lac repressor binding sites. The resulting caveolin-1 wild-type and mutant constructs were confirmed by sequencing. The Polybrene method (Brewer, 1994) was used to transfect CHO-K2 lacRep cells with the indicated construct. The transfected cells were selected with 0.6 mg/ml G418 (GIBCO BRL) over a period of 14 d. After selection, individual clones were isolated by limiting dilution and screened for inducible expression of wild-type or mutant caveolin-1 by immunofluorescence and immunoblotting.

For transient expression of Cav$_{134-178}$, CHO-K2 cells were transiently transfected with the construct using Fugene 6 (Roche) according to the manufacturer protocol.

Immunofluorescence Microscopy

Cells (2×10^5/well) were seeded into individual wells of a 24-well plate containing 12-mm glass coverslips and grown until 50% confluent before the addition of 5 mM IPTG for 16 h. Cells were then fixed in 100% methanol for 5 min at −20°C. The coverslips were sequentially incubated at room temperature in PBS plus 0.5% BSA for 60 min, the indicated primary antibody for 30 min, and the appropriate fluorescent-tagged pAb IgG for 30 min. The coverslips were then mounted on glass slides with Aquamount (Polyscience) and viewed with a Leica TCS-SP Laser scanning microscope.

Fractionation of Triton X-100 Insoluble Membranes

The presence of wild-type and mutant caveolin-1 in Triton X-100 insoluble light membranes was determined using sucrose gradient fractionation. Each dish of cells was washed in ice cold buffer B and then scraped from the dish into 1 ml of buffer C. The cells were further incubated on ice for 20 min before homogenizing the sample with a dounce homogenizer. The homogenates were transferred to a TH641 centrifuge tube and mixed with an equal volume of 2.5 M sucrose. The sample was then overlaid with a 10–30% linear sucrose gradient and centrifuged for 21 h at 29,000 rpm in a Sorval THP 64.1 rotor. Fractions were collected from the top of the gradient and the total protein in each fraction precipitated with TCA. Precipitates were resuspended in SDS-PAGE sample buffer, separated by gel electrophoresis, and immunoblotted with the indicated antibody.

Incorporation of Caveolin-1 into High Molecular Weight Complex

Velocity sedimentation was used to determine if wild-type and mutant caveolin-1 were incorporated into high molecular weight complexes (Sargiacomo et al., 1995). Cells were scraped into buffer D and incubated on ice for 30 min. After removal of cellular debris and nuclei by centrifugation (Eppendorf Microcentrifuge) at 22,000 g for 10 min at 4°C, the supernatant material was loaded on top of a linear 5–30% sucrose gradient and centrifuged for 16 h at 50,000 rpm (340,000 g) in a Beckmann SW-60 rotor.

12 fractions were collected from the top the gradient and the protein precipitated with TCA. Precipitates were resuspended in SDS-PAGE sample buffer, separated by gel electrophoresis and immunoblotted with the indicated antibody.

Protease Protection Assay

The topology of wild-type and mutant caveolin-1 in the membrane was determined as described previously (Smart et al., 1994). Cells from a 100-mm cell culture dish were collected in 1 ml buffer E and homogenized in a Potter Elvjhem homogenizer. The nuclei and unbroken cells were removed by centrifuging the sample at 1,000 g for 10 min at 4°C. The supernatant fraction was centrifuged for 1 h at 100,000 g in a Beckmann 100.3 rotor. The pellet was resuspended in 1 ml buffer A and transferred to microtubes. Each sample was then incubated for 30 min on ice either in buffer alone, 300 μg/ml trypsin, or trypsin plus 1% Triton X-100. The total protein in each sample was precipitated with TCA. Precipitates were resuspended in SDS-PAGE sample buffer, separated by gel electrophoresis, and immunoblotted with the indicated antibody.

Detection of Caveolin-1 Oligomers

To detect caveolin oligomers, IPTG induced cells grown on a 35-mm dish were collected in 200 μl SDS sample buffer and solubilized by sonication (three times 40 J bursts). Without boiling, the samples were separated by SDS-PAGE on a 3–20% gradient gel and immunoblotted with the indicated antibody (Monier et al., 1996).

Immunoblotting

Equal volume fractions were incubated in SDS sample buffer (Laemmli, 1970) at 95°C for 5 min and separated by electrophoresis at 25 mA per gel. The proteins were transferred to polyvinylidene difluoride membranes (Millipore Corp.). After blocking with TBST (20 mM Tris, pH 8.0, 137 mM NaCl, 0.4% Tween 20) containing 5% nonfat dry milk, the membranes were incubated with the first antibody in TBST containing 1% nonfat dry milk followed by the second antibody in TBST containing 1% nonfat dry milk. Bound antibody was detected using an ECL detection system (Amersham Pharmacia Biotech).

Results

The strategy used in this study was to express various mutant forms of Myc-tagged caveolin-1 (listed in Fig. 1) and look at the distribution of the Myc epitope using immunofluorescence, immunoelectron microscopy, and cell fractionation. We used CHO cells stably transfected with an expression plasmid controlled by an IPTG regulated promoter. The CHO cell, which normally expresses caveolin-1, was chosen for these studies so that we could screen for mutant caveolin-1 that might alter the distribution of the endogenous protein or have a dominant-negative effect on caveolae function. More importantly, we wanted to use a cell that was able to properly sort endogenous caveolin-1.

Localization of Mutant Caveolins

We began by expressing the full-length α isoform of caveolin-1 (Fig. 2) and found this Myc-tagged, ectopically expressed protein was primarily at the cell surface in association with the endogenous protein (Cav$_{1-178}$; Fig. 2, A and B). Immunogold labeling of Lowicryl K4M sections confirmed that the Myc epitope was localized to invaginated caveolae (data not shown). The exact same distribution was seen for the 32-aa, shorter β isoform (Cav$_{32-178}$; data not shown). Removing 60 aa from the NH$_2$ terminus did not affect the distribution of the protein (Cav$_{60-178}$; Fig. 2 C), but the loss of an additional 41 aa caused the protein to accumulate in the interior of the cell (Cav$_{101-178}$; Fig. 2 D).
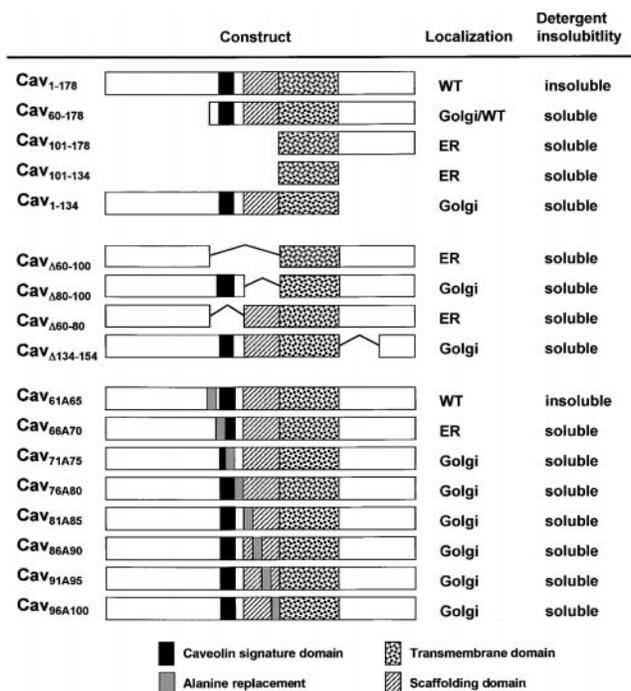

Figure 1. Schematic representation of normal and mutant caveolin-1. The 17 different constructs of caveolin-1 used in this study are depicted as bar diagrams, beginning with wild-type caveolin-1 (Cav$_{1-178}$). Three landmarks in the protein are: the highly conserved signature domain, aa 68–75 (solid box); the scaffolding domain, aa 80–100 (hatched box); and the membrane insertion domain, aa 101–133 (stippled box). The thin connecting line indicates the position of the deleted segment. Eight of the constructs (Cav$_{61A65}$ to Cav$_{96A100}$) have the indicated aa replaced with alanine residues. The location of the alanine substitution in each construct is indicated by the gray box. The columns beside each bar diagram indicates the principal site of accumulation in CHO cells of each construct and whether or not it is soluble in Triton X-100.

The immunofluorescence pattern for Cav$_{101-178}$ suggested it was in the ER and nuclear envelope. Further truncation of the protein by removing the putative membrane insertion site caused it to accumulate in the nuclear envelope and the Golgi region of the cell (Cav$_{134-178}$; Fig. 2, E and F). Cav$_{134-178}$ only partially colocalized with the Golgi marker mannosidase II (compare Fig. 2 E with Fig. 2 F).

Removal of the last 22 aa of caveolin-1 had no effect on its distribution (data not shown). Cav$_{1-134}$, by contrast, colocalized with mannosidase II (Fig. 3, A and B). Cav$_{1-101}$ had a diffuse, cytoplasmic distribution consistent with the behavior of a cytosolic protein (data not shown). Finally, when we removed both the NH$_2$- (aa 1–100) and the COOH-terminal (aa 134–178) portions of the molecule, the remaining 33 aa hydrophobic piece had an ER and nuclear envelope staining pattern (Cav$_{101-134}$; Fig. 3 C).

The behavior of the various truncated caveolins indicates that there are at least two domains within the molecule that influence its intracellular traffic. A region between aa 60 and 101 influences the exit of the protein from the ER, whereas the region between aa 134 and 156 is required for migration from the Golgi apparatus to the cell surface. To gain better resolution of these two controlling
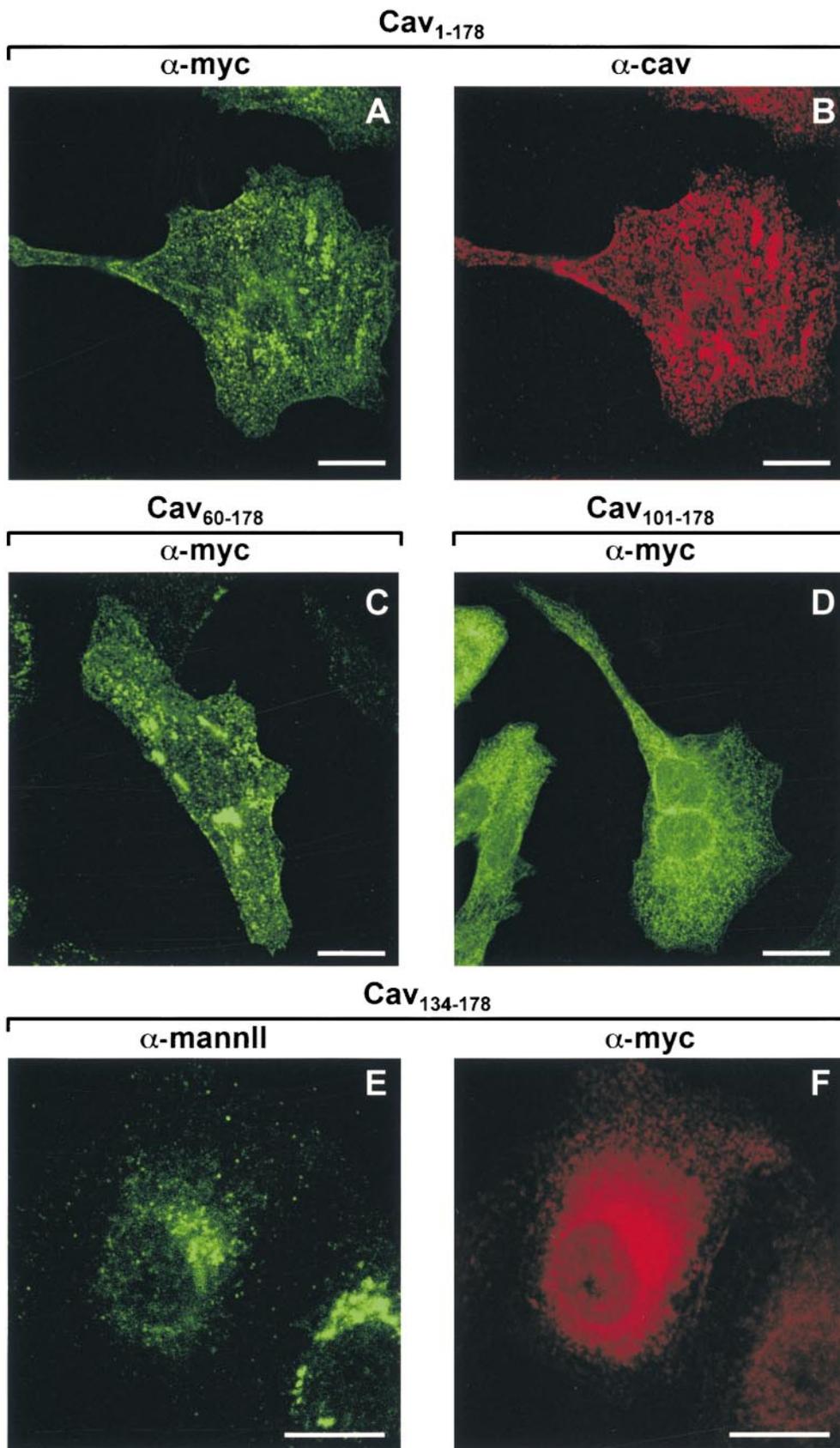
Cav$_{1-178}$

α-myc   A

α-cav   B

Cav$_{60-178}$

α-myc   C

Cav$_{101-178}$

α-myc   D

Cav$_{134-178}$

α-mannII   E

α-myc   F

Figure 2. Location of NH$_2$-terminal deletion mutants of caveolin-1. CHO cells either stably transfected with Myc-tagged forms of Cav$_{1-178}$ (A and B), Cav$_{60-178}$ (C), or Cav$_{101-178}$ (D) under control of an IPTG inducible promoter or transiently transfected with Cav$_{134-178}$ (E and F) were grown on coverslips. Cells were either induced for 16 h with 5 mM IPTG (A–D) or not treated (E and F). CHO cells expressing Cav$_{1-178}$ were costained with Myc pAb (A) and caveolin mAb (B). CHO cells expressing either Cav$_{60-178}$ (C) or Cav$_{101-178}$ (D) were stained with Myc pAb. CHO cells transiently expressing Cav$_{134-178}$ were double-stained with mannosidase II pAb (E) and Myc mAb (F). Bars, 10 μm.
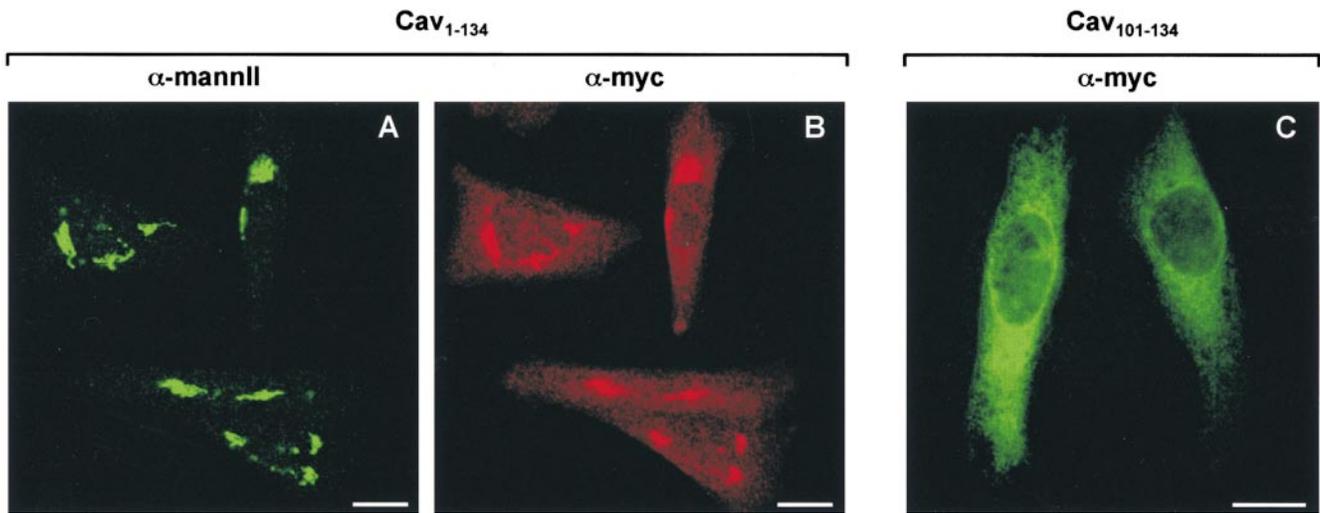
Figure 3. Location of caveolin-1 with COOH-terminal deletions (A and B) and of the membrane insertion domain alone (C). (A and B) CHO cells stably transfected with Myc-tagged Cav_{1-134} were grown on coverslips and induced for 16 h with 5 mM IPTG. Cells were processed for double immunofluorescence labeling with mannosidase II pAb (A) and Myc mAb (B). (C) CHO cells were transiently transfected with Myc-tagged $Cav_{101-134}$ and grown on coverslips for 24 h. Cells were processed for indirect immunofluorescence using Myc pAb. Bars, 10 μm.

elements, we constructed expression vectors coding for proteins that had portions of these regions deleted (Fig. 4). A caveolin-1 lacking aa 60–100 had an ER distribution ($Cav_{\Delta60-100}$; Fig. 4 A), whereas deletion of aa 134–154 gave a Golgi staining pattern ($Cav_{\Delta134-154}$; Fig. 4 D). $Cav_{\Delta60-100}$ colocalized with the ER marker protein BIP (BIP; Fig. 4 B) and $Cav_{\Delta134-154}$ with mannosidase II (mannII; Fig. 4 C). Next we expressed a caveolin-1 with either aa 60–80
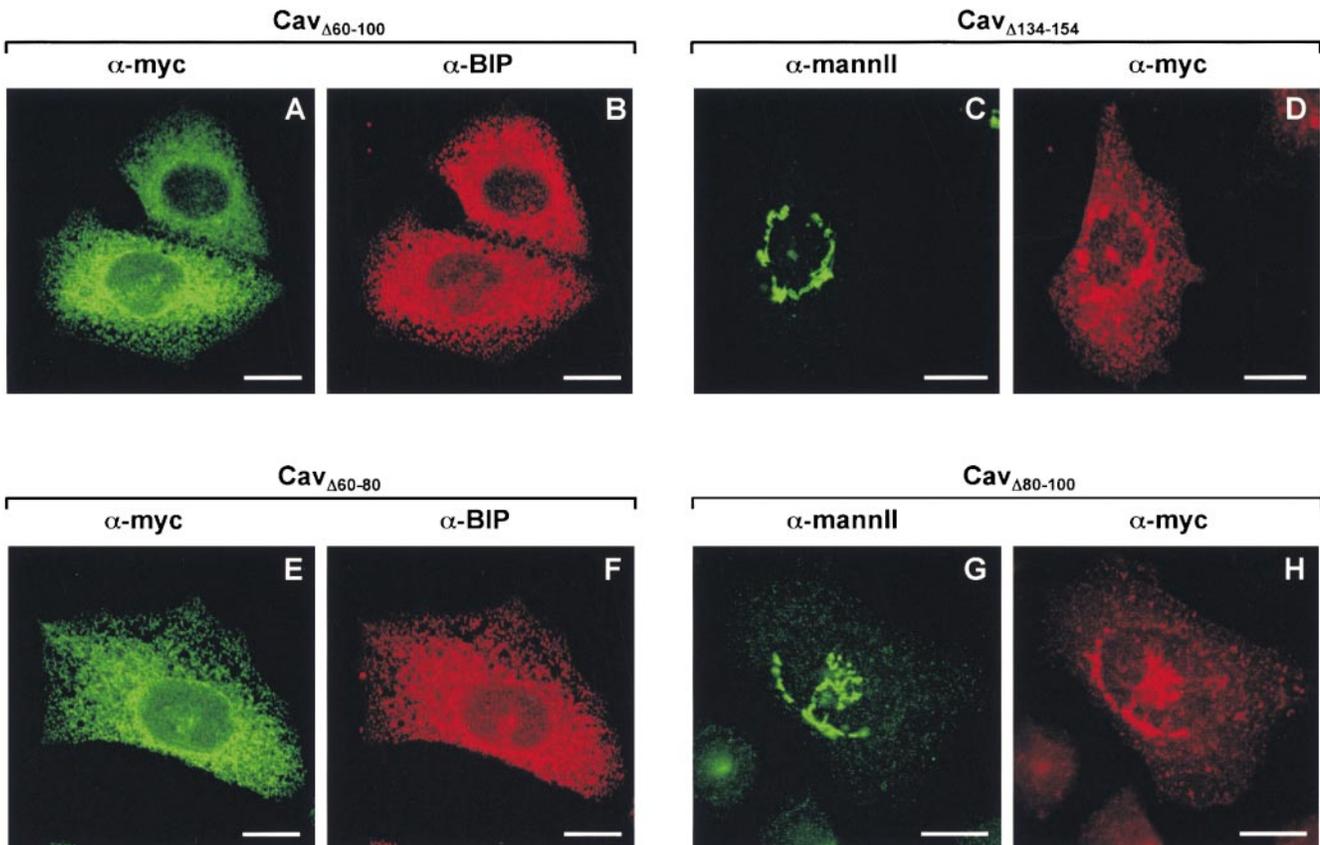

Figure 4. Effect of internal deletions on location of caveolin-1. CHO cells stably transfected with either Myc-tagged $Cav_{\Delta60-100}$ (A and B), $Cav_{\Delta134-154}$ (C and D), $Cav_{\Delta60-80}$ (E and F), or $Cav_{\Delta80-100}$ (G and H) under control of an IPTG inducible promoter were grown on coverslips. Cells were processed for indirect immunofluorescence localization of either the Myc epitope (A, D, E, and H), BIP (B and F), or mannosidase II (C and G). Bars, 10 μm.
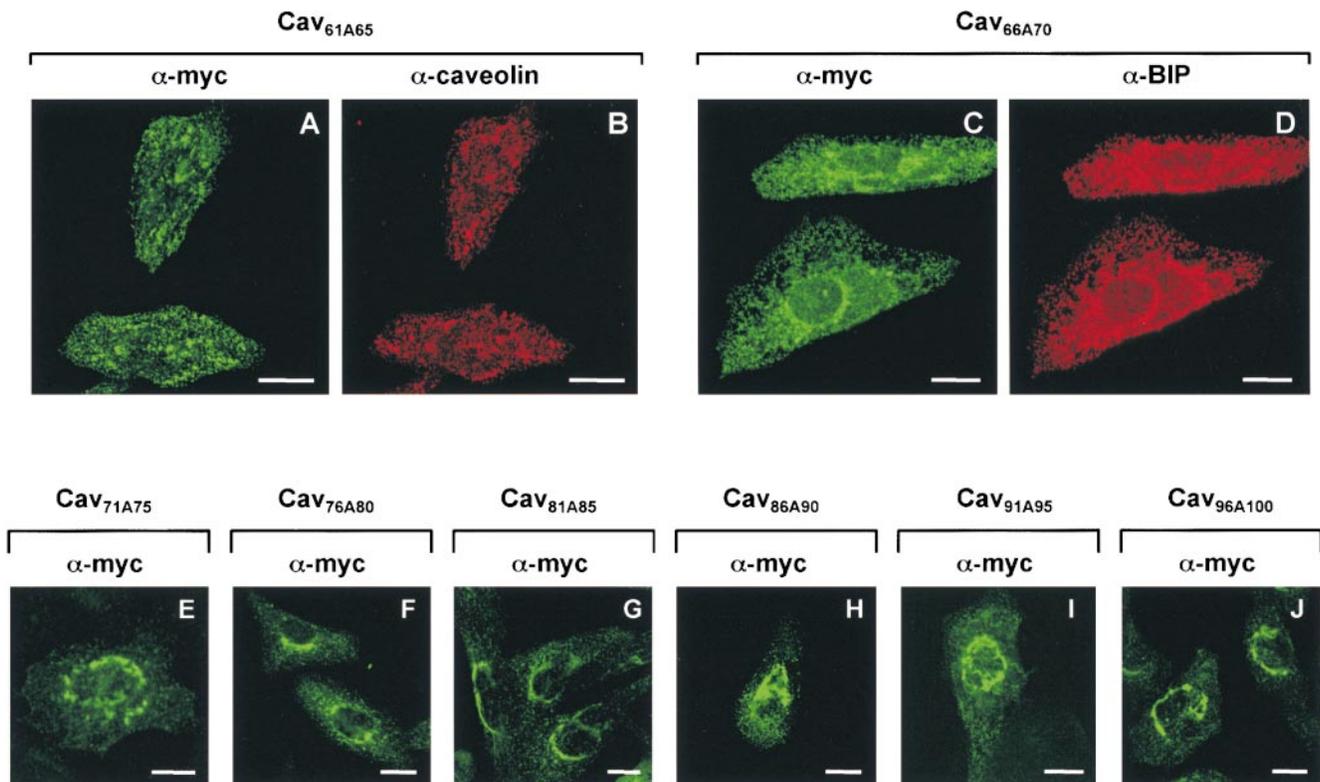
Machleidt et al. *Caveolae, Caveolin-1, Membrane Traffic, Protein Sorting*   21

Figure 5. Effect of alanine-substitution on location of caveolin-1. CHO cells stably transfected with either Myc-tagged Cav_{61A65} (A and B), Cav_{66A70} (C and D), Cav_{71A75} (E), Cav_{76A80} (F), Cav_{81A85} (G), Cav_{86A90} (H), Cav_{91A95} (I), or Cav_{96A100} (J) under control of an IPTG inducible promoter were grown on coverslips in the presence of IPTG for 16 h. Cells were processed for indirect immunofluorescence localization of the Myc epitope (A, C, and E–J), caveolin-1 (B), or BIP (D). Bars, 10 μm.

($Cav_{\Delta 60-80}$; Fig. 4 E) or aa 80–100 removed ($Cav_{\Delta 80-100}$; Fig. 4 H). Interestingly, $Cav_{\Delta 60-80}$ had an ER distribution, whereas $Cav_{\Delta 80-100}$ was only found in the Golgi apparatus. Double immunofluorescence confirmed that $Cav_{\Delta 60-80}$ colocalized with BIP (Fig. 4 F) and $Cav_{\Delta 80-100}$ with mannosidase II (Fig. 4 G). Immunogold EM verified the location of these two constructs (data not shown). Therefore, between aa 60 and 100 there appears to be two trafficking signals, one for transit of caveolin-1 out of the ER and one for movement from the Golgi apparatus to the cell surface.
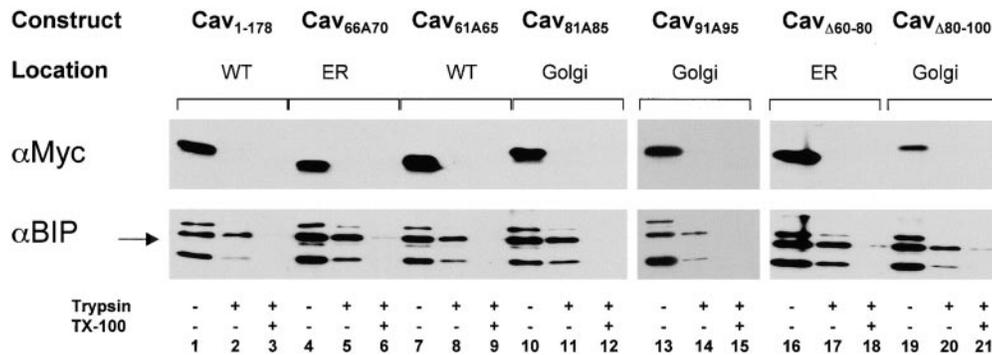
The sequence from aa 68 to 75 is the most conserved segment of the molecule between *C. elegans* and humans (designated the signature domain), whereas the region between aa 80 to 101 is thought to modulate the activity of multiple signal transducing molecules (the scaffolding domain) (Okamoto et al., 1998). We sequentially replaced 5-aa long segments from aa 60 to 101 with alanine residues and analyzed by immunofluorescence the distribution of each mutant form (Fig. 5). Replacing aa 61–65 with alanines had no effect on the distribution of the protein (compare endogenous [Fig. 5 A] with Cav_{61A65} [Fig. 5 B]). By contrast, substitution of the next five aa with alanines caused the protein to accumulate in the ER (compare Cav_{66A70} [Fig. 5 C] with BIP [Fig. 5 D]). Caveolins bearing any of the other substitutions (Cav_{71A75}, Fig. 5 E; Cav_{76A80}, Fig. 5 F; Cav_{81A85}, Fig. 5 G; Cav_{86A90}, Fig. 5 H; Cav_{91A95}, Fig. 5 I; and Cav_{96A100}, Fig. 5 J) primarily had a perinuclear

distribution similar in character to a Golgi pattern of staining.

Organization of Mutant Caveolins in the Cell

The results so far indicate there are three regions in the caveolin-1 molecule that exert control over its intracellular location. The 20-aa long regions on either side of the putative membrane anchor modulates departure from the Golgi apparatus. The five aa between positions 66 and 70 control exit from the ER. To better understand why these mutant forms are not properly localized in the cell, we used a series of biochemical tests that measure the topology and turnover of these proteins as well as their ability to interact with themselves and with other cellular proteins.

When caveolin-1 is in caveolae it behaves like an integral membrane protein oriented with both ends in the cytoplasm (Kurzchalia and Parton, 1996). As a consequence, most of the caveolin-1 in the cell is protease-sensitive, except when it collects in the ER lumen of cells exposed to cholesterol oxidase (Smart et al., 1994). We used protease sensitivity to determine the topology of various mutant caveolins (Fig. 6). Cells expressing either wild-type or the indicated mutant caveolin-1, all tagged with the Myc epitope, were homogenized and high-speed membrane pellets were prepared. The pellet was incubated in the

Construct	Cav$_{1-178}$	Cav$_{66A70}$	Cav$_{61A65}$	Cav$_{81A85}$	Cav$_{91A95}$	Cav$_{\Delta60-80}$	Cav$_{\Delta80-100}$
Location	WT	ER	WT	Golgi	Golgi	ER	Golgi

αMyc

αBIP →

Trypsin	-	+	+	-	+	+	-	+	+	-	+	+	-	+	+	-	+	+	-	+	+
TX-100	-	-	+	-	-	+	-	-	+	-	-	+	-	-	+	-	-	+	-	-	+
	1	2	3	4	5	6	7	8	9	10	11	12	13	14	15	16	17	18	19	20	21

Figure 6. All mutant forms have a wild-type orientation. CHO cells expressing the indicated Myc-tagged caveolin-1 construct were homogenized as described in Materials and Methods. Aliquots of the homogenate were either not treated (lanes 1, 4, 7, 10, 13, 16, and 19), incubated in the presence of 300 μg/ml trypsin for 30 min on ice (lanes 2, 5, 8, 11, 14, 17, and 20), or incubated in the presence of 1% Triton X-100 plus trypsin (lanes 3, 6, 9, 12, 15, 18, and 21). Samples were separated by SDS-PAGE and immunoblotted with Myc pAb.

presence (Fig. 6, lanes 2, 3, 5, 6, 8, 9, 11, 12, 14, 15, 17, 18, 20, and 21) or absence (Fig. 6, lanes 1, 4, 7, 10, 13, 16, and 19) of trypsin or with trypsin plus Triton X-100 (Fig. 6, lanes 3, 6, 9, 12, 15, 18, and 21). The membranes were separated by gel electrophoresis at the end of the incubation and immunoblotted with either pAb Myc or a pAb against the luminal ER protein, BIP (Hebert et al., 1995). Regardless of the mutant form, all of these tagged caveolins were protease-sensitive without the addition of detergents. Most of the BIP, on the other hand, was resistant to protease treatment, indicating that it was protected within the ER lumen. BIP was destroyed by the protease when the membrane was permeabilized with Triton X-100. Similar results were obtained when pAb caveolin-1 was substituted for pAb Myc (data not shown). Therefore, regardless of whether the mutant caveolin-1 was in the ER (Cav$_{\Delta60-80}$, Cav$_{66A70}$), the Golgi apparatus (Cav$_{\Delta80-100}$, Cav$_{91A95}$, Cav$_{81A85}$), or caveolae (Cav$_{61A65}$), it appeared to retain the same orientation as the wild-type protein. This indicates that mutant forms of caveolin-1 would not be able to interact with chaperones in the lumen of either the ER or Golgi apparatus.

Despite having the correct orientation in the membrane, the mislocalized mutant forms of caveolin-1 could be trapped in these locations as a consequence of being partially unfolded. One measure of misfolding is a rapid rate of turnover relative to the wild-type protein. This is because cells have a quality control mechanism that recognizes misfolded ER and cytoplasmic proteins and rapidly shunts them to the ubiquitin/proteasome pathway for degradation (Kopito, 1997). Caveolin-1 has a relatively slow turnover time, so we used immunoblotting to compare the rate of disappearance of Myc-tagged wild-type and mutant caveolin-1 from cells that had been incubated in the presence of cycloheximide (Fig. 7). During an 8-h incubation in the presence of this drug, there was very little loss of wild-type Cav$_{1-178}$ from the cell. Cav$_{\Delta60-80}$, Cav$_{\Delta60-100}$, Cav$_{66A70}$, and Cav$_{61A65}$ were also quite stable. By contrast, the degradation of Cav$_{\Delta80-100}$, Cav$_{81A85}$, Cav$_{96A100}$, and Cav$_{101-178}$ was markedly accelerated. The turnover of both Cav$_{\Delta134-154}$ and Cav$_{71A75}$ was only slightly faster than the

wild-type protein. Therefore, there appears to be no correlation between where individual mutant caveolins accumulate in the cell and their rate of turnover. To the extent that rapid degradation measures misfolding, the Cav$_{66A70}$

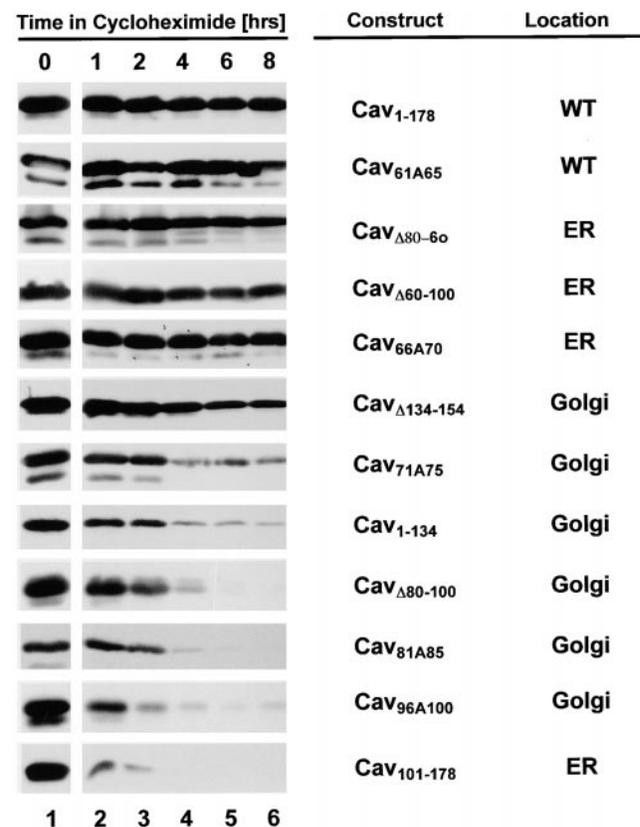| Time in Cycloheximide [hrs]						Construct	Location
0	1	2	4	6	8		
						Cav$_{1-178}$	WT
						Cav$_{61A65}$	WT
						Cav$_{\Delta80-60}$	ER
						Cav$_{\Delta60-100}$	ER
						Cav$_{66A70}$	ER
						Cav$_{\Delta134-154}$	Golgi
						Cav$_{71A75}$	Golgi
						Cav$_{1-134}$	Golgi
						Cav$_{\Delta80-100}$	Golgi
						Cav$_{81A85}$	Golgi
						Cav$_{96A100}$	Golgi
						Cav$_{101-178}$	ER
1	2	3	4	5	6		

Figure 7. Turnover of wild-type and mutant caveolin-1. CHO cells stably expressing the indicated Myc-tagged caveolin-1 construct were either not treated (lane 1) or incubated in the presence of 500 μM cycloheximide for 1 (lane 2), 2 (lane 3), 4 (lane 4), 6 (lane 5), or 8 h (lane 6). At the end of the incubation, the cells were lysed, separated by SDS-PAGE, and immunoblotted with Myc pAb. The table indicates the predominant location of the construct as determined by immunofluorescence.

in the ER and the $Cav_{\Delta134-154}$ in the Golgi apparatus seem to have relatively normal conformations.

Several studies indicate that the caveolin-1 in caveolae forms a high molecular weight complex with itself and with caveolin-2 (Das et al., 1999). Other proteins may be in the complex as well. We used velocity sedimentation to determine if any of the mutant forms of caveolin-1 were impaired in complex formation (Fig. 8). Cells expressing each construct were solubilized in octylglucoside and centrifuged at low speed to remove nuclei and cellular debris. The supernatant fraction was loaded on the top of a 5–30% sucrose gradient containing 60 μM octylglucoside and centrifuged at 340,000 g for 16 h. 12 fractions were collected from the top of the gradient, separated by gel electrophoresis, and immunoblotted. The wild-type and the mutant caveolins that traffic normally to the cell surface were all found in complexes that sediment to the bottom of the gradient (Cav_{endo}, Cav_{1-178}, Cav_{60-178}, and Cav_{61A65}). The ER-located $Cav_{\Delta60-100}$ was not in a complex nor were the Golgi-located $Cav_{\Delta60-100}$, Cav_{91A95}, Cav_{96A100}, and Cav_{1-134}. The ER-associated Cav_{66A70} and the Golgi-associated Cav_{81A85} and Cav_{86A90} only partially localized to complexes. Surprisingly, the Cav_{71A75} and Cav_{76A80}, which both accumulate in the Golgi apparatus, were exclusively in the high molecular weight region of the gradient. Therefore, the ability of caveolin-1 to assemble into high molecular weight complexes may be necessary to reach the cell surface, but it is not sufficient.

High molecular weight complexes of caveolin-1 are often seen migrating at the top of SDS polyacrylamide gels after electrophoresis. We used SDS-PAGE to determine how the mutant caveolins migrated (Fig. 9). Samples of membranes from cells induced to express wild-type and mutant caveolin-1 were separated by SDS gel electrophoresis and immunoblotted with pAb Myc. Oligomeric α- (Fig. 9, lane 1) and β-caveolin-1 (Fig. 9, lane 2) appeared as prominent bands on the gel. As observed previously (Monier et al., 1995), more of the β isoform was oligomerized than the α isoform relative to the amount of monomer on the gel. $Cav_{\Delta60-80}$ (Fig. 9, lane 5) and $Cav_{\Delta80-100}$ (Fig. 9, lane 4) did not form any oligomer, nor did $Cav_{\Delta134-154}$ (Fig. 9, lane 3). Whereas the introduction of alanine residues between aa 65 to 71 (Fig. 9, lane 7) and 90 to 101 (Fig. 9, lane 10) completely abolished oligomerization, oligomer formation was normal for Cav_{61A65} (Fig. 9, lane 6) and Cav_{71A75} (Fig. 9, lane 8). The amount of oligomer formed by the Cav_{81A85} (Fig. 9, lane 9) mutant was intermediate between wild-type and $Cav_{\Delta80-100}$. Therefore, both the sedimentation and the SDS-PAGE assay agree that specific mutations impair the ability of caveolin-1 to form high molecular weight complexes.

Caveolin-1 oligomer formation is associated with the incorporation of the molecule into detergent resistant, light membranes (Scheiffele et al., 1998). These membranes tend to form in the Golgi apparatus (Brown and Rose, 1992; Lisanti et al., 1993). We used a standard assay to measure the ability of wild-type and mutant forms of caveolin-1 to float on sucrose gradients after Triton X-100 treatment of whole cells. Cells expressing the indicated constructs were homogenized in Triton X-100, layered on the bottom of a sucrose gradient, and centrifuged at 29,000 g for 21 h. (Fig. 10). Equal volume fractions were
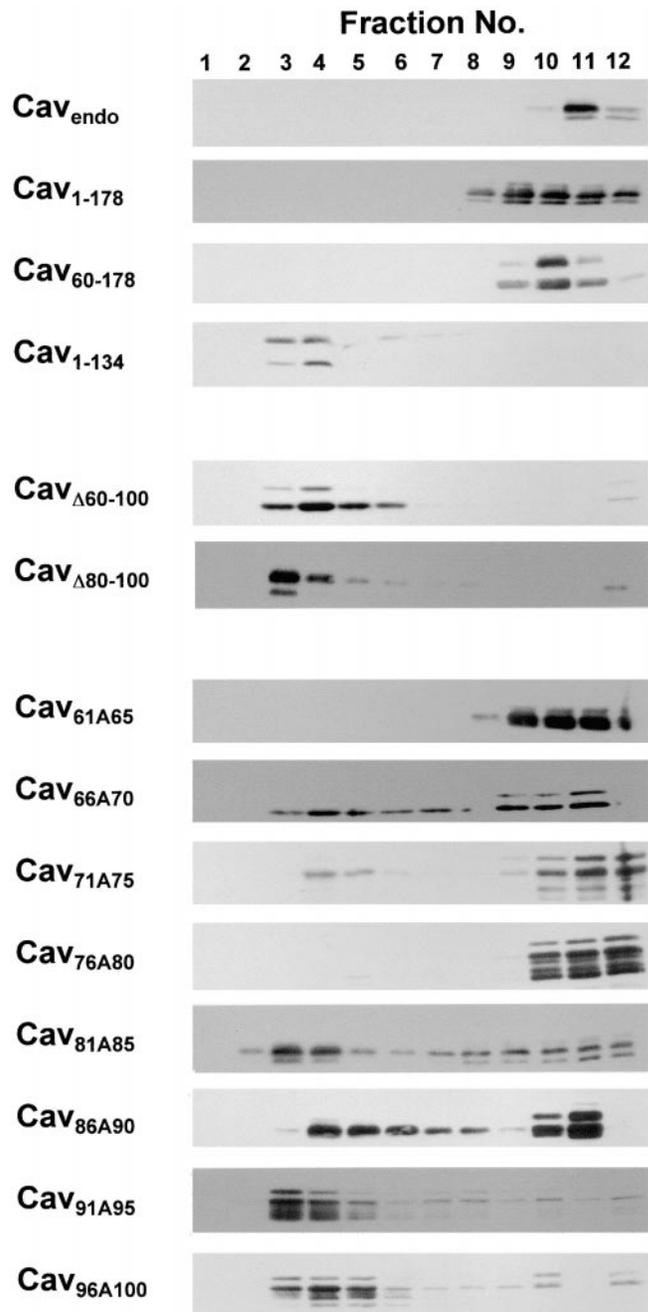

Figure 8. Ability of wild-type and mutant caveolin-1 to form high molecular complexes. CHO cells or CHO cells stably expressing the indicated Myc-tagged caveolin-1 construct were extracted with buffer containing 60 mM octylglucoside. The lysate was loaded on the top of a 5–30% continuous sucrose gradient and centrifuged for 16 h at 340,000 g. Fractions were collected from the top of the gradient, separated by gel electrophoresis, and immunoblotted with either a caveolin-1 pAb (Cav_{endo}) or Myc pAb (Cav_{1-178} to Cav_{95A100}).

separated by gel electrophoresis and immunoblotted with either pAb Myc or pAb caveolin-1. Endogenous caveolin-1 (Cav_{endo}) quantitatively floated in fractions 5–9, indicating that nearly all of the protein was incorporated into Triton X-100 insoluble light membranes. All of the Myc-tagged, wild-type caveolin-1 was in this fraction too. However,
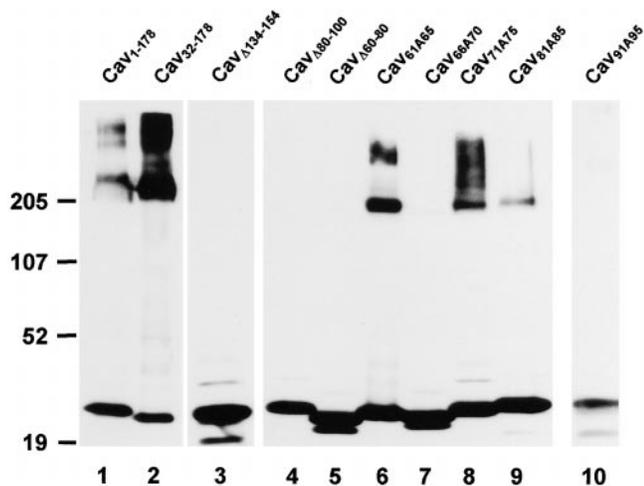
24

Figure 9. Ability of wild-type and mutant caveolin-1 to form oligomers. Samples of CHO cells expressing the indicated Myc-tagged caveolin construct were collected in sample buffer containing 2% (wt/vol) SDS and 5% (vol/vol) 2-β-mercaptoethanol and solubilized by sonication. Samples were separated on 3–20% polyacrylamide gradient gels and immunoblotted with Myc pAb.

with the exception of Cav_{61A65}, none of the mutant caveolins floated in these fractions. Even Cav_{71A75} and Cav_{76A80}, which are able to oligomerize, were not incorporated into Triton X-100 insoluble light membranes.

Discussion

In previous studies, mutagenesis has been used to identify functional elements of caveolin. The key discoveries that have come from this approach include: the isolation of a dominant-negative acting form of caveolin-3 (Roy et al., 1999); the identification of a region in caveolin-1 that interacts with multiple signaling molecules (Okamoto et al., 1998); the identification of regions in caveolin-1 that affect vesicle formation in Sf21 cells (Li et al., 1996) and control homo-oligomerization (Song et al., 1997; Li et al., 1998); and the identification of a putative Golgi apparatus targeting sequence in caveolin-3 (Luetterforst et al., 1999). These investigations have employed a variety of in vitro and in vivo techniques as well as used diverse cellular systems to express the normal and mutant forms. As a consequence, it is sometimes difficult to relate the results of each study to the normal behavior of caveolin-1 in the cell. The goal of this study was to understand the molecular basis of caveolin-1 sorting as the molecule moves through various membrane compartments. The success of this analysis depended on using a cell that was actively processing and properly sorting the protein. Therefore, we introduced normal and mutant Myc-tagged forms of caveolin-1 into cells expressing the endogenous protein. Although it is possible that interactions between the expressed protein and endogenous caveolin-1 masked crucial sorting information, we were still able to identify four regions of the molecule that are involved in sorting caveolin-1 during its transit through ER and Golgi membranes. Three of these regions are involved in sorting
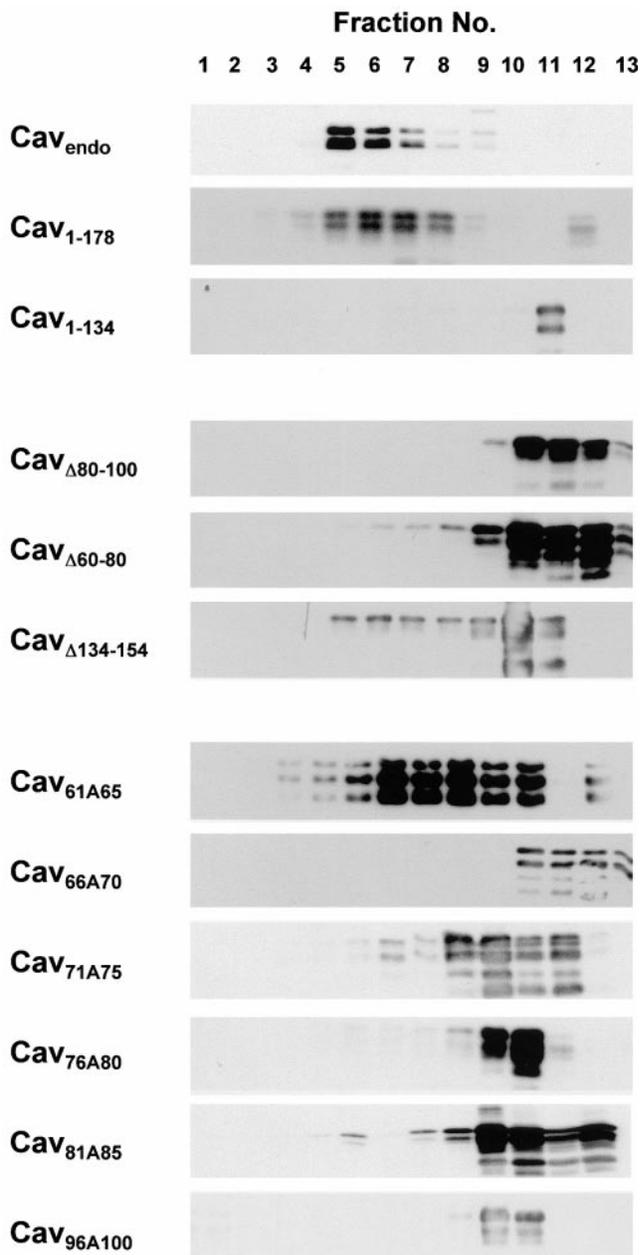

Figure 10. Ability of wild-type and mutant caveolin-1 to incorporate into Triton X-100 insoluble, light membranes. CHO cells or CHO cells stably expressing the indicated Myc-tagged caveolin-1 construct were extracted with 1% Triton X-100 at 4°C overlaid with a 10–30% sucrose gradient. The detergent insoluble fraction was separated from the soluble fraction by centrifugation at 29,000 rpm for 21 h. The gradient was fractionated from the top (fraction 1). Equal volumes of each fraction were separated by SDS-PAGE and immunoblotted with either caveolin-1 pAb (Cav_{endo}) or Myc pAb (Cav_{1-178} to Cav_{96A100}) as described.

events that occur in the Golgi apparatus, whereas the fourth operates during sorting from the ER.

Accumulation in the ER

Replacing the 5-aa long segment $_{66}IDFED_{70}$ with alanine residues causes caveolin-1 to accumulate in the ER.

A homologous sequence is present in both caveolin-2 ($_{51}$LGFED$_{55}$) and caveolin-3 ($_{39}$VDFED$_{43}$) and they all are at similar positions in the molecule. Based on the results of several tests, caveolin-1 with this mutation is correctly oriented in the membrane, is not rapidly shunted into a degradation pathway, and is poorly oligomerized. These properties suggest the mutant caveolin-1 originates by cotranslational insertion into the membrane (Monier et al., 1995), but does not relocate to the Golgi apparatus. Either it moves to the Golgi apparatus but is rapidly returned or it is unable to exit from the ER.

We can think of two mechanisms to account for this behavior. Either an interaction between the IDFED sequence and an unidentified factor(s) is required to relocate caveolin-1 to the Golgi apparatus, or the replacement of this sequence with alanine residues causes retention in the ER due to improper folding. We favor the first mechanism. The 33-aa hydrophobic domain (Cav$_{101-134}$) tagged with the Myc epitope accumulated in the ER exactly like Cav$_{66A70}$. This construct does not have any cytoplasmic regions, so retention in the ER due to an interaction with chaperones is unlikely. The simple addition of the NH$_2$-terminal 100 aa of caveolin-1 to this peptide (Cav$_{1-134}$) allowed the hydrophobic region to move, along with the NH$_2$-terminal tail, to the Golgi apparatus. The results of the mutagenesis and truncation experiments indicate that there are no other regions between aa 1 and 101 that influence movement from the ER. Therefore, the IDFED sequence appears to be sufficient to move the caveolin-1 membrane insertion domain out of the ER. It is likely to regulate the relocation of the full-length protein too.

Accumulation in the Golgi Apparatus

The region between aa 71 and 101 contains information that influences the passage of caveolin-1 through the Golgi apparatus. This sequence contains the putative scaffolding domain (aa 81–101) and a portion of the highly conserved region we call the signature domain (aa 68–75). Even though mutations in both regions caused caveolin-1 to accumulate in the Golgi apparatus, we detected distinct differences in the behavior of the two sets of mutant molecules.

Caveolin-1 begins to oligomerize shortly after being synthesized in the ER (Scheiffele et al., 1998). The size of the caveolin-1 oligomer increases and becomes more Triton X-100 insoluble as the complex moves to the cell surface (Scheiffele et al., 1998). Triton X-100 insolubility appears to begin in the Golgi apparatus along with the association of caveolin-1 complexes with glycosylphosphatidylinositol (GPI) anchored proteins (Lisanti et al., 1993). Previous work has identified the region between aa 60 and 101 as being involved in an oligomerization step (Sargiacomo et al., 1995). We found that substitution of alanine residues for any of the aa between 70 and 80 had no effect on oligomerization. However, the oligomers that formed were soluble in Triton X-100. We also found by immunogold labeling that caveolin-1 bearing alanine substitutions in this region were distributed throughout the Golgi apparatus (data not shown). These results raise the possibility that in the Golgi apparatus, oligomerization precedes entry into cholesterol/glycosphingolipid-rich membranes. If this is

the case, then a function for the signature domain might be to control access to cholesterol/glycosphingolipid-rich membranes. This may be a critical step during the traffic of all caveolins, because the $_{68}$FEDVIAEP$_{75}$ sequence is the longest conserved stretch of aa among the three isoforms.

Substituting sets of five alanine residues anywhere along the 20-aa stretch between position 80 and 100 interferes with caveolin-1 oligomerization. We saw the most complete effect when the residues between 90 and 101 were replaced with alanine. 6 of the 10 residues in this region are hydrophobic and 5 of these are aromatic. aa 89 is also aromatic. Therefore, the hydrophobicity of this region may be a critical factor in controlling caveolin-1 oligomerization. We also found that caveolins with alanine substitutions in $_{91}$TFTVTKYWFY$_{100}$ were Triton X-100 soluble. This is consistent with recent studies showing that caveolin 1–101 interacts with Triton X-100 insoluble, light membrane fractions, but caveolin 1–81 does not (Schlegel et al., 1999). Caveolin-1 with alanine substitutions in $_{71}$VIAEPEGTHS$_{80}$ was also Triton X-100 soluble and contains a normal $_{91}$TFTVTKYWFY$_{100}$. This is further evidence that the $_{71}$VIAEPEGTHS$_{80}$ region controls access to Triton X-100 insoluble membrane domains. Otherwise, caveolin-1 with alanine substitutions in this region should be Triton X-100 insoluble. However, the question remains whether caveolin-1 with mutations in the $_{91}$TFTVTKYWFY$_{100}$ sequence ever reaches cholesterol/glycosphingolipid-rich membranes in the Golgi apparatus. These mutant caveolins accumulate in the Golgi apparatus either because they cannot reach these domains or are unable to remain bound during vesicle formation.

The fourth region of caveolin-1 that controls sorting is the sequence between aa 134 and 154. Caveolin-1 lacking the entire COOH-terminal region (Cav$_{1-134}$) accumulated in the Golgi apparatus but was completely soluble in Triton X-100 and unable to incorporate into high molecular weight complexes. 12 of the 20 aa between 134 and 154 are hydrophobic, and a cysteine residue at position 143 most likely is palmitoylated (Dietzen et al., 1995). When we deleted this region, the mutant caveolin-1 also accumulated in the Golgi apparatus. Removal of aa 157–178 had no effect on sorting. Cav$_{\Delta134-154}$ was unable to oligomerize but did partially associate with Triton X-100 insoluble, light membranes. Apparently, caveolin-1 oligomerization depends on both aa 90–99 and 134–154. Interestingly, Song et al. (1997) found that Cav$_{1-140}$ was able to oligomerize normally. This result suggests the sequence $_{135}$KSFLIE$_{140}$ may be the region that influences oligomerization between aa 134 and 154. Therefore, two sequences, one on each side of the 33 membrane insertion domain, appear to act cooperatively during caveolin-1 oligomerization.

Other Insights

There is now growing evidence that the intracellular travel itinerary for caveolin-1 varies according to the cell type. For example, caveolin-1 expressed in fibroblasts and some epithelial cells is found principally in caveolae and the Golgi apparatus (Kurzchalia et al., 1992; Rothberg et al., 1992), whereas in pancreatic acinar cells it is targeted to the secretory pathway (Liu et al., 1999). The focus of the current study has been on the behavior of Myc-tagged ca-

veolins in fibroblasts that express and sort caveolin-1 to caveolae. Three observations we made using this cell background do not agree with published reports on the behavior of mutant caveolin-3 expressed in fibroblasts. First, we found that Cav_{60-178} was delivered rather efficiently to the cell surface. The equivalent sequence of caveolin-3 (Cav_{54-151}) expressed in CV1 cells accumulates in the Golgi apparatus (Luetterforst et al., 1999) and in vesicular structures that have the characteristics of lipid droplets (Roy et al., 1999). Second, we found that caveolin-1 lacking the COOH-terminal cytoplasmic region between aa 134–178 accumulated in the Golgi apparatus, whereas an equivalent construct of caveolin-3 (aa 1–107) seems to be retained in the ER of CV1 cells (Luetterforst et al., 1999). Finally, we found no evidence that the COOH-terminal cytoplasmic portion of caveolin-1 contains a domain for targeting the molecule to the Golgi apparatus (Luetterforst et al., 1999). To the contrary, deletion of aa 134–154 caused caveolin-1 to accumulate in the Golgi apparatus, indicating that without this region the molecule is impaired in reaching the surface. In contrast, caveolin-1 lacking aa 154–178 behaved like the wild-type molecule. Most likely, $Cav_{\Delta134-154}$ accumulates in the Golgi apparatus because oligomerization is necessary for rapid movement to the cell surface and oligomer formation is dependent on this stretch of hydrophobic aa.

The behavior of the various mutant forms of caveolin-1 we analyzed suggests the wild-type molecule is synthesized as a membrane protein in the ER and then moves sequentially through various compartments on its way to the cell surface. The four different mutant forms that acted aberrantly were unable to move through one of these compartments at a normal pace. In most instances, the mislocalization cannot be explained by an inappropriate interaction with endogenous caveolin-1, because the traffic of the endogenous protein was relatively normal. The proper traffic of caveolin-1, therefore, relies on intramolecular cues that are necessary for the molecule to travel through specific membrane compartments.

References

Anderson, R.G.W. 1998. The caveolae membrane system. *Annu. Rev. Biochem.* 67:199–225.

Brewer, C.B. 1994. Cytomegalovirus plasmid vectors for permanent lines of polarized epithelial cells. *Methods Cell Biol.* 43:233–245.

Brown, D.A., and J.K. Rose. 1992. Sorting of GPI-anchored proteins to glycolipid-enriched membrane subdomains during transport to the apical cell surface. *Cell.* 68:533–544.

Conrad, P.A., E.J. Smart, Y.-S. Ying, R.G.W. Anderson, and G.S. Bloom. 1995. Caveolin cycles between plasma membrane caveolae and the Golgi complex by microtubule-dependent and microtubule-independent steps. *J. Cell Biol.* 131:1424–1433.

Das, K., R.Y. Lewis, P.E. Scherer, and M.P. Lisanti. 1999. The membrane-spanning domains of caveolins-1 and -2 mediate the formation of caveolin hetero-oligomers. Implications for the assembly of caveolae membranes in vivo. *J. Biol. Chem.* 274:18721–18728.

Dietzen, D.J., W.R. Hastings, and D.M. Lublin. 1995. Caveolin is palmitoylated on multiple cysteine residues. Palmitoylation is not necessary for localization of caveolin to caveolae. *J. Biol. Chem.* 270:6838–6842.

Fielding, C.J., A. Bist, and P.E. Fielding. 1997. Caveolin mRNA levels are up-regulated by free cholesterol and down-regulated by oxysterols in fibroblast monolayers. *Proc. Natl. Acad. Sci. USA.* 94:3753–3758.

Fra, A.M., E. Williamson, K. Simons, and R.G. Parton. 1995. De novo formation of caveolae in lymphocytes by expression of VIP21-caveolin. *Proc. Natl. Acad. Sci. USA.* 92:8655–8659.

Glenney, J.R. 1989. Tyrosine phosphorylation of a 22-kDa protein is correlated with transformation by Rous sarcoma virus. *J. Biol. Chem.* 264:20163–20166.

Glenney, J.R., and L. Zokas. 1989. Novel tyrosine kinase substrates from Rous sarcoma virus-transformed cells are present in the membrane skeleton. *J. Cell Biol.* 108:2401–2408.

Hailstones, D., L.S. Sleer, R.G. Parton, and K.K. Stanley. 1998. Regulation of caveolin and caveolae by cholesterol in MDCK cells. *J. Lipid Res.* 39:369–379.

Hebert, D.N., J.F. Simons, J.R. Peterson, and A. Helenius. 1995. Calnexin, calreticulin, and Bip/Kar2p in protein folding. *Cold Spring Harbor Symp. Quant. Biol.* 60:405–415.

Kopito, R.R. 1997. ER quality control: the cytoplasmic connection. *Cell.* 88:427–430.

Kurzchalia, T.V., and R.G. Parton. 1996. And still they are moving . . . . dynamic properties of caveolae. *FEBS Lett.* 389:52–54.

Kurzchalia, T.V., P. Dupree, R.G. Parton, R. Kellner, H. Virta, M. Lehnert, and K. Simons. 1992. VIP21, a 21-kD membrane protein is an integral component of trans-Golgi-network–derived transport vesicles. *J. Cell Biol.* 118:1003–1014.

Laemmli, U.K. 1970. Cleavage of structural proteins during the assembly of the head of bacteriophage T4. *Nature.* 227:680–685.

Li, S., K.S. Song, S.S. Koh, A. Kikuchi, and M.P. Lisanti. 1996. Baculovirus-based expression of mammalian caveolin in Sf21 insect cells. A model system for the biochemical and morphological study of caveolae biogenesis. *J. Biol. Chem.* 271:28647–28654.

Li, S., F. Galbiati, D. Volonte, M. Sargiacomo, J.A. Engelman, K. Das, P.E. Scherer, and M.P. Lisanti. 1998. Mutational analysis of caveolin-induced vesicle formation. Expression of caveolin-1 recruits caveolin-2 to caveolae membranes. *FEBS Lett.* 434:127–134.

Lisanti, M.P., Z. Tang, and M. Sargiacomo. 1993. Caveolin forms a hetero-oligomeric protein complex that interacts with an apical GPI-linked protein: implications for the biogenesis of caveolae. *J. Cell Biol.* 123:595–604.

Liu, P., W.-P. Li, T. Machleidt, and R.G.W. Anderson. 1999. Identification of caveolin-1 in lipoprotein particles secreted by exocrine cells. *Nat. Cell Biol.* 1:369–375.

Luetterforst, R., E. Stang, N. Zorzi, A. Carozzi, M. Way, and R.G. Parton. 1999. Molecular characterization of caveolin association with the Golgi complex: identification of a cis-Golgi targeting domain in the caveolin molecule. *J. Cell Biol.* 145:1443–1459.

Mineo, C., G.N. Gill, and R.G.W. Anderson. 1999. Regulated migration of EGF receptors from caveolae. *J. Biol. Chem.* 274:30636–30643.

Monier, S., R.G. Parton, F. Vogel, J. Behlke, A. Henske, and T.V. Kurzchalia. 1995. VIP21-caveolin, a membrane protein constituent of the caveolar coat, oligomerizes in vivo and in vitro. *Mol. Biol. Cell.* 6:911–927.

Monier, S., D.J. Dietzen, W.R. Hastings, D.M. Lublin, and T.V. Kurzchalia. 1996. Oligomerization of Vip21-caveolin in vitro is stabilized by long chain fatty acylation or cholesterol. *FEBS Lett.* 388:143–149.

Murata, M., J. Peränen, R. Schreiner, F. Wieland, T.V. Kurzchalia, and K. Simons. 1995. VIP21/caveolin is a cholesterol-binding protein. *Proc. Natl. Acad. Sci. USA.* 92:10339–10343.

Okamoto, T., A. Schlegel, P.E. Scherer, and M.P. Lisanti. 1998. Caveolins, a family of scaffolding proteins for organizing "preassembled signaling complexes" at the plasma membrane. *J. Biol. Chem.* 273:5419–5422.

Parton, R.G., B. Joggerst, and K. Simons. 1994. Regulated internalization of caveolae. *J. Cell Biol.* 127:1199–1215.

Rothberg, K.G., J.E. Heuser, W.C. Donzell, Y.-S. Ying, J.R. Glenney, and R.G.W. Anderson. 1992. Caveolin, a protein component of caveolae membrane coats. *Cell.* 68:673–682.

Roy, S., R. Lutterforst, A. Harding, A. Apolloni, M. Etheridge, E. Stang, B. Rolls, J.F. Hancock, and R.G. Parton. 1999. Dominant-negative caveolin inhibits H-Ras function by disrupting cholesterol-rich plasma membrane domains. *Nat. Cell Biol.* 1:98–105.

Sargiacomo, M., P.E. Scherer, Z. Tang, E. Kubler, K.S. Song, M.C. Sanders, and M.P. Lisanti. 1995. Oligomeric structure of caveolin: implications for caveolae membrane organization. *Proc. Natl. Acad. Sci. USA.* 92:9407–9411.

Scheiffele, P., P. Verkade, A.M. Fra, H. Virta, K. Simons, and E. Ikonen. 1998. Caveolin-1 and -2 in the exocytic pathway of MDCK cells. *J. Cell Biol.* 140:795–806.

Schlegel, A., R.B. Schwab, P.E. Scherer, and M.P. Lisanti. 1999. A role for the caveolin scaffolding domain in mediating the membrane attachment of caveolin-1. The caveolin scaffolding domain is both necessary and sufficient for membrane binding in vitro. *J. Biol. Chem.* 274:22660–22667.

Smart, E.J., Y.-U. Ying, P.A. Conrad, and R.G.W. Anderson. 1994. Caveolin moves from caveolae to the Golgi apparatus in response to cholesterol oxidation. *J. Cell Biol.* 127:1185–1197.

Smart, E.J., Y.-S. Ying, W.C. Donzell, and R.G.W. Anderson. 1996. A role for caveolin in transport of cholesterol from ER to plasma membrane. *J. Biol.*

Chem. 271:29427–29435.

Song, K.S., Z. Tang, S. Li, and M.P. Lisanti. 1997. Mutational analysis of the properties of caveolin-1. A novel role for the C-terminal domain in mediating homo-typic caveolin-caveolin interactions. *J. Biol. Chem.* 272:4398–4403.

Trigatti, B.L., R.G. Anderson, and G.E. Gerber. 1999. Identification of caveolin-1 as a fatty acid binding protein. *Biochem. Biophys. Res. Commun.* 255: 34–39.

Uittenbogaard, A., Y. Ying, and E.J. Smart. 1998. Characterization of a cytoso-lic heat-shock protein-caveolin chaperone complex. Involvement in cholesterol trafficking. *J. Biol. Chem.* 273:6525–6532.

Wary, K.K., F. Mainiero, S.J. Isakoff, E.E. Marcantonio, and F.G. Giancotti. 1996. The adaptor protein Shc couples a class of integrins to the control of cell cycle progression. *Cell.* 87:733–743.

Welch, H., A. Eguinoa, L.R. Stephens, and P.T. Hawkins. 1998. Protein kinase B and rac are activated in parallel within a phosphatidylinositide 3OH-kinase-controlled signaling pathway. *J. Biol. Chem.* 273:11248–11256.